Synthesis of Solketal from glycerol catalyzed by spherical γ-Al 2 O 3 supported FeCl 3

Tiantian Zhang
Beijing Technology and Business University
Shan Liao
Beijing Technology and Business University
Xiulan Xin (xinxl2007@126.com)
Beijing Technology and Business University
Hongqin Liu
Beijing Technology and Business University
Yang Yu
Beijing Technology and Business University
Baocai Xu
Beijing Technology and Business University

Research Article

Keywords: Mesoporous structure, Glycerol acetalization, Solketal, FeCl3/γ-Al2O3, Fuel additives

Posted Date: October 21st, 2022

DOI: https://doi.org/10.21203/rs.3.rs-2173222/v1

Abstract

The porous spherical alumina (γ-Al_2O_3) as catalyst support was prepared by sol-gel method, and $FeCl_3$/γ-Al_2O_3 materials were prepared by impregnation method. The $FeCl_3$/γ-Al_2O_3 materials were used as catalyst in the Solketal production process by acetalization of acetone and glycerol, showing considerable catalytic performance. When the molar ratio of glycerol and acetone was 1:10, 0.2 mol% $FeCl_3$/γ-Al_2O_3 was used as the catalyst, and the reaction was carried out at 25°C for 30 min, the conversion of glycerol was 99.89%, the selectivity of Solketal was 98.36%, and the yield of Solketal reached 98.25%. The mechanism is due to the spherical γ-Al_2O_3 support has high thermal stability, large specific surface area, and rich pore structure, encouraging abundant active sites and high catalytic activity of $FeCl_3$ for the acetalization reaction. Thereafter, the experimental results prove that the prepared $FeCl_3$/γ-Al_2O_3 catalyst can be easily recovered and reused many times, indicating its great value for large-scale research and application in the future.

1. Introduction

With the massive consumption of fossil fuels and serious environmental pollution, exploring clean and renewable biomass fuel is of great importance for the future development of global economy [1–3]. Biodiesel is one of the most promising biomass fuel and has been commercialized for agricultural production, power generation machinery, public transportation, and shipping vessels [4]. However, a huge amount of the glycerol by-products is formed (ca. 10%) during the production process of biodiesel, resulting in a serious resource waste [5]. Recently, it was found that glycerol can be used as a raw material to synthesize biodiesel additives, showing a new and effective route to achieve the conversion and utilization of waste glycerol into high value-added chemical products [6, 7]. For example, 2,2-dimethyl-1,3-dioxolane-4-methanol (a solvent type branched chain oxygenated compound, also named as Solketal) can be obtained by acetalization of acetone and glycerol and directly used as solvent, low-temperature heat transfer fluid, surfactants or fuel additives [8–10]. In addition, a six membered ring product (6MR, 2,2-dimethyl-1,3-dioxane-5-ol) can also be produced (Scheme 1) [11].

Importantly, the preparation of Solketal by acetalization of acetone and glycerol is under the action of catalyst. Inorganic acids (*e.g.*, HCl, H_2SO_4) are commonly used catalysts most early but show strong corrosiveness, poor thermal stability and non-recyclability [12–16]. Solid catalysts (*e.g.*, zeolite [17], niobium oxide [11], zirconium oxide [4], supported heteropoly acid [18], sulfonated resin [19] and carbon-based acid catalyst [20, 21]) can overcome above disadvantages of liquid catalysts and are once thought to be promising substitutes for inorganic acids [13, 22]. Unfortunately, as a homogeneous catalyst, the solid catalysts exhibit severely acid site leaching and phase change. More seriously, the formed water during the acetalization process inactivates Lewis and Bronsted acid sites [5, 23]. The construction of heterogeneous acid catalysts and the design of catalyst supports have become a research hotspot in recent years [10, 24]. For example, Y-type zeolite-based catalysts have become one of the most commonly used catalysts due to their unique structure, acidity, low cost, and high thermal stability [25].

However, the hydrophobicity of the zeolite as the catalyst support severely limits its catalytic performance [26]. Besides the hydrophilia, the micro- and meso-pore structure of catalyst support is benefit to the heterogeneous catalyst for glycerol acetalization. Considering that the reactant molecules are generally transported to the active sites of the catalyst through the mesoporous channels and the diameter of the acetalization product is 0.43–0.51 nm [23], spherical porous γ-Al_2O_3 with large specific surface area and developed mesopores may be an rational choice for the catalyst support. Furthermore, the acetalization reaction of Solketal is an equilibrium reaction with a low equilibrium constant, and the removal of by-product H_2O can effectively improve the reaction degree [27]. Generally, desiccants (*e.g.*, sodium sulfate, potassium carbonate or phosphorus pentoxide, etc.) can remove H_2O from Solketal but the practical process requires much time and effort [28]. Benefitting from the good water absorption ability, spherical γ-Al_2O_3 is conducive to the forward progress of the equilibrium reaction. The literature has described the continuous formation of ketals using heterogeneous catalysts [29], such as commercial macroporous acid resins of the Amberlyst family. Vicente *et al*. reported the applicability of mesosulfonate silica as a catalyst for the acetalization of glycerol [5]. Devaki Nandan *et al*. developed a simple, single-step, template-free, simultaneous carbonization and sulfonation method, using glucose as carbon source and template precursor, and discussed the applicability of the acidic sulfonated carbon–silica-meso composite material obtained in the synthesis of phenolic resin in industry [30]. However, up to now, there are few reports on the use of spherical γ-Al_2O_3 for this catalytic reaction.

On the other hand, Iron chloride is an inexpensive Lewis acid catalyst, which has recently been reported for green acetalization of glycerol with various carbonyl compounds. G. Arellano *et al*. found that even if a very small amount of iron (0.63 wt.%) was incorporated, the catalytic performance of the aluminosilicate catalyst for the acetalization glycerol was greatly improved [31]. Homogeneous iron salts are non-toxic, inexpensive and environmentally friendly, and have absolute single-point catalysis, showing great value of practical application [32]. S. Zaher *et al*. reported a new type of iron alginate as a cheap and environmentally friendly catalyst for the production of ketone from glycerol and acetone [33]. The low price, good affordability and high Lewis acidity of iron (III) salt make it a counter ion in heteropoly acid salt, which is widely used in this catalytic reaction [34–36]. Silva D. et al [37] also revealed the positive effect of homogeneous Fe(III) catalyst on the reaction. Overall, the unprecedented high activity, low load (up to 10 ppm), good ecotoxicological characteristics, and high activities of iron salt are expected to become convincing catalysts for the sustainable transformation of renewable by-products in nontoxic solvents [38–41]. Therefore, combining the advantages of spherical porous γ-Al_2O_3 as support and Iron chloride as catalyst may achieve comprehensive catalyst performance for the acetalization of acetone and glycerol.

Herein, we prepared γ-Al_2O_3 by sol-gel method using various ball washing solvents, further synthesized $FeCl_3$/γ-Al_2O_3 catalyst by the impregnation method using γ-Al_2O_3 as the support for the first time. Thereafter, Solketal is synthesized by solvent-free method using glycerol and acetone as raw materials and $FeCl_3$/γ-Al_2O_3 as catalyst. Through the optimization of reaction temperature, reaction time, molar ratio of reactants, catalyst amount and other parameters, the best glycerol conversion rate and selectivity

to Solketal were obtained. The results showed that the prepared solid acid catalyst had mild reaction conditions, high stability, high product yield, good selectivity, and low pollution, revealing the great potential of $FeCl_3$/γ-Al_2O_3 as the catalyst for the reaction between glycerol and acetone.

2. Experimental

2.1. Preparation of γ-Al_2O_3

For a standard synthesis, 30.63 g aluminum isopropoxide and 55.29 g distilled water were added into a three-necked flask to completely hydrolysis. Then, 11.76 mL dilute nitric acid (1 mol/L) was added and gel aged in a certain temperature for a certain time to obtain an aluminum sol with the certain viscosity. Spherical γ-Al_2O_3 precursor was prepared by oil-ammonia column shaping method and washed by water, methanol, ethanol, isopropanol, n-butanol, isoamyl alcohol, n-hexanol and n-octanol, respectively. After drying at room temperature (25 ± 1 ℃) for 24 h further 110 ℃ for 8 h, and calcination followed at 600 ℃ for 4 h, the obtained spherical γ-Al_2O_3 were named γ-Al_2O_3-H_2O, γ-Al_2O_3-MT, γ-Al_2O_3-EA, γ-Al_2O_3-IPA, γ-Al_2O_3-NBA, γ-Al_2O_3-IAA, γ-Al_2O_3-HA, γ-Al_2O_3-CA, respectively.

2.2. Characterization Of γ-alo

The thermal behavior of precursor was investigated by thermal gravimetric analysis (TGA) and differential thermal (DTG) analysis (MS3000, Mettler Toledo, China). The Zeiss Sigma 300 microscope (Zeiss, Germany) was used for scanning electron microscopy (SEM) analysis to observe the macroporous structure. The acceleration voltage was 1 kV. The nitrogen isotherm adsorption measurements were performed on the fully automatic ratio scale and calibration analyzer (ASAP 2460, USA). The transmission electron microscope (TEM, JEM-2100, Japan) was used to characterize the microstructure and explore the microscopic composition of the sample. Bruker Axs X-ray diffractometer (XRD, Germany) was used to test the crystal structure of spherical Al_2O_3. The test range was 2θ at 10–80°. Cu Kα radiation was used as the X-ray source. The functional groups were characterized by Nicolet Avatar 370 Fourier transform infrared spectrometer (FTIR), and the test range was 400–4000 cm^{-1}. The sample was thoroughly mixed with dry KBr powder and pressed into a disc for measurements. The digital microscope was used to photograph the spherical γ-Al_2O_3, and the sphericity was calculated after the diameter measured.

The bulk density was obtained by the ratio of weight (M, g) and volume (V, cm^3) using a cylinder mold.

The compressive strength was investigated by intelligent particle strength testing machine analysis (ZQJ-II, China).

2.3. Preparation Of Fecl/γ-alo

$FeCl_3$/γ-Al_2O_3 catalyst was prepared by impregnation method. Typically, certain amounts of $FeCl_3$ and spherical γ-Al_2O_3 were added in 10 mL H_2O (the mole percent of $FeCl_3$ in the catalyst is 0.1-1 mol%). After stirring at room temperature for 24 h, the impregnated spherical γ-Al_2O_3 was directly dried at 110°C for 3 h and calcined at 300°C for 2 h. Finally, the $FeCl_3$/γ-Al_2O_3 catalysts were obtained and named as $FeCl_3$/γ-Al_2O_3-H_2O, $FeCl_3$/γ-Al_2O_3-MT, $FeCl_3$/γ-Al_2O_3-EA, $FeCl_3$/γ-Al_2O_3-IPA, $FeCl_3$/γ-Al_2O_3-NBA, $FeCl_3$/γ-Al_2O_3-IAA, $FeCl_3$/γ-Al_2O_3-HA, $FeCl_3$/γ-Al_2O_3-CA, respectively.

2.4. Characterization Of Fecl/γ-alo

Energy dispersive spectrometer (EDS) analysis was performed using a Zeiss Sigma 300 microscope at an acceleration voltage of 10 kV (Zeiss, Germany). The microstructure was characterized by transmission electron microscope (TEM, JEM-2100, Japan).

2.5. Catalytic Activity Measurement

Glycerol acetalization was carried out in a round bottom flask equipped with a water-cooled condenser. Typically, 0.92 g glycerol and 5.81 g acetone (molar ratio is 1: 10) and 0.2 mol% $FeCl_3$/γ-Al_2O_3 catalyst were slowly added into the flask with magnetically stirring. It was reacted at 25°C for 30 min. Thereafter, 100 μL of the reaction mixture was removed to 1.5 mL gas phase bottle to be analyzed by GC-MS(Agilent-7890A-7000B) equipped with HP-5 capillary column (30 m × 0.32 mm × 0.25 μm). Meanwhile, $FeCl_3$/γ-Al_2O_3 catalyst was recovered from the reaction system by separation, washing and calcination at 300°C for 2 h to remove adsorbed H_2O and organic matter. The glycerol conversion and Solketal selectivity were gotten based on the following equations:

$$\mathrm{Conversionofglycerol}\,(\%) = \left(1 - \frac{\mathrm{Areaofunreactedglycerol}}{\mathrm{Initialareaofglycerol}}\right) \times 100\%$$

$$\mathrm{SelectivityofSolketal}\,(\%) = \frac{\mathrm{AreaofSolketal}}{\mathrm{AreaofSolketal} + \mathrm{Areaofacetal}} \times 100\%$$

$$\mathrm{YieldofSolketal}\,(\%) = \mathrm{Conversionofglycerol} \times \mathrm{SelectivityofSolketal} \times 100\%$$

3. Results And Discussion

3.1. Structural characterization of γ-Al_2O_3

We first characterized the thermal stability of the various γ-Al_2O_3 precursors obtained by different washed solvents to choose a rational calcination temperature. The precursors of γ-Al_2O_3-H_2O, γ-Al_2O_3-MT, γ-Al_2O_3-EA, γ-Al_2O_3-IPA, γ-Al_2O_3-NBA, γ-Al_2O_3-IAA, γ-Al_2O_3-HA, and γ-Al_2O_3-CA are named as AlOOH-H_2O, AlOOH-MT, AlOOH-EA, AlOOH-IPA, AlOOH-NBA, AlOOH-IAA, AlOOH-HA, and AlOOH-CA, respectively. And their TGA

and DTG curves are displayed in Fig. 1, all showing three distinct thermal decomposition steps. (1) The decomposition of free water begins at ca. 100°C with a mass loss of 10%; (2) the -OH and organic componence decompose at 200–500°C and the content is *ca.* 20%; and (3) the mass loss of *ca.* 2% during 500–600°C is attributed to the crystal transformation. We realize from the almost constant mass of the samples above 600°C that is the optimal calcination temperature. The precursors all exhibit weight loses of 30%-40% during the calcination process (Table 1), which is in accordant with the TG results.

Table 1
Weight loss data of the precursors.

	AlOOH-H_2O	AlOOH-MT	AlOOH-EA	AlOOH-IPA	AlOOH-NBA	AlOOH-IAA	AlOOH-HA	AlOOH-CA
25–800°C	35.11	33.96	33.36	34.03	33.62	33.69	35.69	38.17
25–200°C	9.51	10.74	11.00	10.85	10.72	10.95	10.63	11.72
200–500°C	22.88	21.11	20.49	21.27	20.75	20.72	22.99	23.45
500–800°C	2.76	2.16	1.93	1.97	2.19	2.06	2.12	3.09

The XRD patterns (Fig. 2a) of the obtained spherical γ-Al_2O_3 samples after calcination all show three typical diffraction peaks located at (311), (400) and (440), revealing their γ-Al_2O_3 structure (JCPDS no.29–0063). Noticeably, inferred from the similar intensity of the peaks of all samples, the crystal structure of the spherical γ-Al_2O_3 is no related to the types of the washed solvent. According to the Scherrer formula ($D = (K\gamma) / (B \cdot \cos\theta)$), (K is the Scherrer constant, 0.89, D is the average thickness of the grain perpendicular to the crystal plane, B is the full width at half maximum of the diffraction peak, θ is the diffraction angle, γ is the X-ray wavelength, 0.154056 nm), the grain size of the spherical γ-Al_2O_3 (440) crystal plane was about 4 nm.

The functional group structure of the spherical γ-Al_2O_3 was tested by FTIR (Fig. 2b). All samples show a wide absorption peak at 3700 – 3300 cm^{-1}, corresponding to -OH and H_2O. The small peak near 1660 cm^{-1} and the broad band at 900 – 500 cm^{-1} are caused by the bending vibration of H-O-H [42] and the stretching vibration of Al-O-Al in bulk phase, respectively. These peaks of the samples exhibit similar intensity, indicating that the washing solvent are not affect their composition and structure.

TEM (Fig. 3) images show that the samples are all composed with the nanorods and the regular and order microscopic particles are stacked to form regular meso- and macro-pores. N_2 adsorption–desorption experiments are conducted to get more information of the pore structure (Fig. 4a). The hysteresis loops of the samples at the relative pressure of 0.6–0.9 reveal their mesopore structure, which

are consistent with the concentrated pore size distribution at 2–20 nm (Fig. 4b). In addition, it can be seen from the SEM images (Fig. 5) that the samples all have large pore structure.

The detailed physical parameters are given in Table 2. The γ-Al_2O_3 all are spheres with a diameter of *ca.* 2 mm and exhibit larger specific surface area, developed mesopores, low bulk density, and high compressive strength, which may provide a tri-functions as catalysis support. (1) The sphere shape is suitable for serving as supports due to their uniform bulk structure and easy recovery operation, which can effectively solve the problem of solid powder catalyst cannot be recycled (such as $FeCl_3$). (2) The enriched pores may provide more active sites for the catalytic reaction, which is beneficial to the progress of the reaction. And (3) the high compressive strength is important for repeated utilization and resources saving.

Table 2
Characteristics of the texture and physical nature of the various spherical γ-Al_2O_3.

Sample	Diameter (mm)	S_{BET}[a] (m^2/g)	PV[b] (cm^3/g)	PS[c] (nm)	Bulk Density (g/mL)	CS[d], (N)
γ-Al_2O_3-H_2O	1.93	248.75	0.44	5.66	0.84	141.4
γ-Al_2O_3-MT	1.98	250.89	0.41	5.45	0.89	126.4
γ-Al_2O_3-EA	2.01	258.86	0.44	5.43	0.85	173.4
γ-Al_2O_3-IPA	1.97	271.88	0.47	5.42	0.83	129.2
γ-Al_2O_3-NBA	2.02	259.70	0.51	6.35	0.88	103.7
γ-Al_2O_3-IAA	2.01	255.54	0.50	6.40	0.91	79.6
γ-Al_2O_3-HA	2.13	302.47	1.04	12.06	0.77	50.9
γ-Al_2O_3-CA	2.28	287.35	0.97	11.39	0.48	21.7
[a]BET specific surface area, [b]PV pore volume, [c]PS pore size, [d]CS Compressive Strength						

3.2. Structural Characterization Of Fecl/γ-alo

To reveal the practical application potential of above 8 kinds of spherical γ-Al_2O_3 for catalyst support, we prepared various $FeCl_3$/γ-Al_2O_3 with $FeCl_3$ as catalyst. First, we characterized the samples by TEM and EDS to observe the $FeCl_3$ distribution in spherical γ-Al_2O_3 using $FeCl_3$/γ-Al_2O_3-IPA as an exemplification (Fig. 6). The obvious black spots are randomly distributed in the γ-Al_2O_3 matrix (Fig. 6a), indicating the

successful load of $FeCl_3$. The result can be further confirmed by the amounts of Fe element in the EDS image (Fig. 6b-d).

3.3. Catalytic Tests

3.3.1. Acetalization of glycerol with acetone

The catalytic performance of the eight $FeCl_3/\gamma\text{-}Al_2O_3$ catalysts with different spherical $\gamma\text{-}Al_2O_3$ as supports for the acetalization of glycerol and acetone is further measured. The measurement is carried out at 25°C for 30 min with a glycerol and acetone molar ratio of 1: 5 and 10 mol% $FeCl_3/\gamma\text{-}Al_2O_3$ catalyst (the mole percent of $FeCl_3$ in the catalyst is 10%). The specific catalytic data are shown in Table 3. It can be found that there was no catalytic performance without adding a catalyst or supporting $FeCl_3$. In addition, among all the samples, the $FeCl_3/\gamma\text{-}Al_2O_3$-IPA material obtained the highest glycerol conversion rate of 94.20%. The reason may be due to its large specific surface area provides sufficient active sites. What's more, $FeCl_3/\gamma\text{-}Al_2O_3\text{-}H_2O$, $FeCl_3/\gamma\text{-}Al_2O_3$-EA, $FeCl_3/\gamma\text{-}Al_2O_3$-IPA and $FeCl_3/\gamma\text{-}Al_2O_3$-HA all show considerable Solketal selectivity of 100%. Above all, $FeCl_3/\gamma\text{-}Al_2O_3$-IPA show an optimal comprehensive performance that not only has the highest conversion rate of glycerol and the yield of Solketal, but also shows high compressive strength (Table 2). Therefore, we choose $\gamma\text{-}Al_2O_3$-IPA as the most promising catalyst for practical application.

Table 3
Glycerol conversions, Solketal yield and selectivity of the acetalization reaction of acetone and glycerol by various catalysts.

Catalyst	Glycerol Conversion (%)	Selectivity (%)		Solketal Yield (%)
		Solketal	dioxane	
Blank test	0	0	0	0
γ-Al_2O_3-IPA	29.13	0	100	0
$FeCl_3$/γ-Al_2O_3-H_2O	80.36	100	0	80.36
$FeCl_3$/γ-Al_2O_3-MT	81.37	97.8	2.2	79.58
$FeCl_3$/γ-Al_2O_3-EA	90.89	100	0	90.89
$FeCl_3$/γ-Al_2O_3-IPA	94.20	100	0	94.20
$FeCl_3$/γ-Al_2O_3-NBA	91.03	99.25	0.75	90.35
$FeCl_3$/γ-Al_2O_3-IAA	86.55	98.47	1.53	85.23
$FeCl_3$/γ-Al_2O_3-HA	78.23	100	0	78.23
$FeCl_3$/γ-Al_2O_3-CA	79.89	97.88	2.12	78.20

To investigate the optimal catalytic condition of $FeCl_3$/γ-Al_2O_3-IPA for the acetalization reaction, we performed single variable experiment as shown in Fig. 7. First, we find the catalytic reaction is almost independent of the reaction temperature (25–100 ℃) because the glycerol conversions still are 100% and the Solketal selectivity are also higher than 98% (Fig. 7a). Thereafter, the effect of reaction time on the catalytic reaction is also studied. When the catalytic reaction is carried out for 30 min, the glycerol conversions reached the highest value of 99.89% with a considerable Solketal selectivity of 98.36% (Fig. 7b). The reason is due to the reverse reaction rate is greater than the forward reaction rate after 30 min. Therefore, we further set a certain reaction temperature (ambient temperature of 25 ℃) and time (30 min) to explore the effect of glycerol and acetone molar ratio and the $FeCl_3$ load on the glycerol conversions, Solketal selectivity, and Solketal yield of the acetalization reaction.

Figure 7c shows that the increased molar ratio of glycerol and acetone generates an enhanced catalytic activity, thus the glycerol conversion gradually increased from 47.30% of 1: 1, to 100% of 1: 20 with an increased Solketal selectivity from 90.60–98.64%. Noticeably, when the molar ratio increase from 1: 10 to 1: 20, the glycerol conversion and Solketal selectivity only increase by 0.11% and 0.28%, respectively. Therefore, we choose 1: 10 as the optimal molar ratio thanks to the low cost. Finally, the effect of the amount of $FeCl_3$ load on the catalytic activity is carried out (Fig. 7d). The glycerol conversions maintain 100% with the increase of $FeCl_3$ load from 0.1 to 1 mol%. When the $FeCl_3$ load increased from 0.1 to 0.2

mol%, the Solketal selectivity increased from 82.39–98.84%, indicating that the addition of catalyst species is conducive to the improvement of catalytic performance. However, catalytic performance can't be continuously enhanced after that is higher than 0.2 due to the sufficient catalyst for limited reactant.

Above all, the optimal reaction conditions are: 25°C reaction temperature, 30 min reaction time, 1: 10 molar ratio of glycerol and acetone, and 0.2 mol% $FeCl_3$/γ-Al_2O_3-IPA catalyst. The glycerol conversion, Solketal selectivity, and Solketal yield are 99.89%, 98.36%, and 98.25%, respectively. The separation and reusability of catalysts are greatly significant for commercialization and environment friendly. Under optimal reaction circumstances, the recovery performance of $FeCl_3$/γ-Al_2O_3-IPA is investigated (Fig. 8). The glycerol conversion nearly unchanged and the Solketal selectivity only show a minor drop of Solketal selectivity after six recycle. The experimental results of re-impregnating $FeCl_3$ for the catalytic process revealed that it may be reused at least six times without losing substantial activity. Inductively Coupled Plasma Optical Emission Spectrometer further reveals there are seldom Fe in the solution, demonstrating the practical recoverability of this catalyst.

4. Conclusion

In conclusion, we prepare various $FeCl_3$/γ-Al_2O_3 as catalyst for the acetalization of glycerol and acetone. γ-Al_2O_3 are synthesized by sol-gel method by different washing solvents, and $FeCl_3$/γ-Al_2O_3 catalysts are further prepared by impregnation method. The catalysts are characterized by XRD, FTIR, BET, SEM, etc, revealing their high thermal stability, large specific surface area and rich pore structure. $FeCl_3$/γ-Al_2O_3-IPA is used as a representative catalyst for the acetalization reaction. When carried out in an optimized experimental conditions that 25°C reaction temperature, 30 min reaction time, 1: 10 molar ratio of glycerol and acetone, and 0.2 mol% $FeCl_3$ load, the glycerol conversion and Solketal selectivity are 99.89% and 98.36%, respectively. Importantly, the catalyst could be reused for at least six reaction cycles without loss of catalytic activity, demonstrated its great value for practical application.

Declarations

Conflicts of interest

There are no conflicts to declare.

Acknowledgements

This work was supported by * Beijing Municipal Science and Technology Project * (grant D17110500190000).

References

1. Miao, Z., et al., Ordered mesoporous titanium phosphate material: A highly efficient, robust and reusable solid acid catalyst for acetalization of glycerol. Chemical Engineering Journal, 2020. 381. Doi.org/10.1016/j.cej.2019.122594
2. Lee, A.F., et al., Heterogeneous catalysis for sustainable biodiesel production via esterification and transesterification. Chemical Society Reviews, 2014. 43(22): p. 7887-916. Doi: 10.1039/c4cs00189c
3. Guo, M., et al., Bioenergy and biofuels: History, status, and perspective. Renewable and Sustainable Energy Reviews, 2015. 42: p. 712-725. Doi.org/10.1016/j.rser.2014.10.013
4. Reddy, P.S., et al., Acetalisation of glycerol with acetone over zirconia and promoted zirconia catalysts under mild reaction conditions. Journal of Industrial and Engineering Chemistry, 2011. 17(3): p. 377-381. Doi: 10.1016/j.jiec.2011.05.008
5. Vicente, G., et al., Acetalisation of bio-glycerol with acetone to produce Solketal over sulfonic mesostructured silicas. Green Chemistry, 2010. 12(5): p. 899-907. Doi: 10.1039/b923681c
6. Dehkhoda, A.M., et al., Biochar based solid acid catalyst for biodiesel production. Applied Catalysis A: General, 2010. 382: p. 197-204. Doi: 10.1016/j.apcata.2010.04.051
7. Mallesham, B., et al., Design of highly efficient Mo and W promoted SnO_2 solid acids for heterogeneous catalysis: acetalization of bio-glycerol. Green Chemistry, 2013. 15(2): p. 478-489. Doi: 10.1039/c2gc36152c
8. Katarzyna, S., et al., The role of bronsted and lewis acid sites in acetalization of glycerol over modified mesoporous cellular foams. The Journal of Physical Chemistry C, 2016. 120: p. 16699-16711. Doi: 10.1021/acs.jpcc.6b04229
9. Timofeeva, M.N., et al., Effect of nitric acid modification of montmorillonite clay on synthesis of Solketal from glycerol, and acetone. Catalysis Communications, 2017. 90: p. 65-69. Doi: 10.1016/j.catcom.2016.11.020
10. Abreu, T.H., et al., Acidic V-MCM-41 catalysts for the liquid-phase ketalization of glycerol with acetone. Microporous and Mesoporous Materials, 2019. 273: p. 219-225. Doi.org/10.1016/j.micromeso.2018.07.006
11. Rodrigues, R., et al., Acetalization of acetone with glycerol catalyzed by niobium-aluminum mixed oxides synthesized by a sol-gel process. Journal of Molecular Catalysis A: Chemical, 2016. 422: p. 122-130. Doi.org/10.1016/j.molcata.2016.02.002
12. Rossa, V., et al., Reaction kinetic study of Solketal production from glycerol ketalization with acetone. Industrial & Engineering Chemistry Research, 2017. 56(2): p. 479-488. Doi: 10.1021/acs.iecr.6b03581
13. Carvalho, B. F., et al., Amphiphilic acid carbon catalysts produced by bio-oil sulfonation for solvent-free glycerol ketalization. Fuel, 2020. 274: p. 117799. Doi.org/10.1016/j.fuel.2020.117799
14. Kowalska, K.J., et al., Enhancement of the catalytic activity of H-ZSM-5 zeolites for glycerol acetalization by mechanical grinding. Reaction Kinetics, Mechanisms and Catalysis, 2015. 117(1): p. 341-352. Doi: 10.1007/s11144-015-0922-4

15. Fatimah, I., et al., Glycerol to Solketal for fuel additive: Recent progress in heterogeneous catalysts. Energies, 2019. 12(15): p. 2872-2886. Doi: 10.3390/en12152872
16. Feliczak, G.A. et al., Application of glycerol to synthesis of solvo-surfactants by using mesoporous materials containing niobium. Microporous and Mesoporous Materials, 2019. 277: p. 301-308. Doi.org/10.1016/j.micromeso.2018.11.008
17. Carolina, X., et al., Water-tolerant zeolite catalyst for the acetalisation of glycerol. Green Chemistry, 2009. 11: p. 38-41. Doi: 10.1039/b813564a
18. Chen, L., et al., Glycerol acetalization with formaldehyde using heteropolyacid salts supported on mesostructured silica. Applied Catalysis A: General, 2018. 549: p. 207-215. Doi.org/10.1016/j.apcata.2017.09.027
19. Barbaro, P., et al., Ion exchange resins: catalyst recovery and recycle. Chemical Reviews, 2009. 109: p. 515-529. Doi: 10.1021/cr800404j
20. Rodrigues, R., et al., Solvent-free conversion of glycerol to Solketal catalysed by activated carbons functionalised with acid groups. Catalysis Science & Technology, 2014. 4(8): p. 2293-2301. Doi: 10.1039/c4cy00181h
21. Goncalves, M., et al., Highly selective acetalization of glycerol with acetone to Solketal over acidic carbon-based catalysts from biodiesel waste. Fuel, 2016. 181: p. 46-54. Doi.org/10.1016/j.fuel.2016.04.083
22. Manjunathan, P., et al., Room temperature synthesis of Solketal from acetalization of glycerol with acetone: Effect of crystallite size and the role of acidity of beta zeolite. Journal of Molecular Catalysis a Chemical, 2015. 396: p. 47-54. Doi.org/10.1016/j.molcata.2014.09.028
23. Talebian, K., et al., Hierarchical faujasite zeolite-supported heteropoly acid catalyst for acetalization of crude-glycerol to fuel additives. Journal of Industrial and Engineering Chemistry, 2019. 79: p. 452-464. Doi.org/10.1016/j.jiec.2019.07.021
24. Gomes, I.S., et al., On the reasons for deactivation of titanate nanotubes with metals catalysts in the acetalization of glycerol with acetone. Chemical Engineering Journal, 2018. 334: p. 1927-1942. Doi.org/10.1016/j.cej.2017.11.112
25. Primo, A. et al., Zeolites as catalysts in oil refining. Chemical Society Reviews, 2014. 43(22): p. 7548-61. Doi: 10.1039/c3cs60394f
26. Kuźniarska, B., et al., Catalytic behavior of 1-(2-pyridylazo)-2-naphthol transition metal complexes encapsulated in Y zeolite. Journal of Catalysis, 2011. 278(1): p. 102-110. Doi: 10.1016/j.jcat.2010.11.022
27. Taddeo, F., et al., Kinetic modeling of Solketal synthesis from glycerol and acetone catalyzed by an iron(III) complex. Catalysts, 2021. 11(1): p. 83-95. Doi.org/10.3390/catal11010083
28. Alsawalha, M., Catalytic activity and kinetic modeling of various modules hzms-5 and treated mcm-41 catalysts, for the liquid-phase ketalization of glycerol with acetone. Frontiers in Chemistry, 2019. 7: p. 799. Doi: 10.3389/fchem.2019.00799

29. Deutsch, J., et al., Investigations on heterogeneously catalysed condensations of glycerol to cyclic acetals. Journal of Catalysis, 2007. 245(2): p. 428-435. Doi: 10.1016/j.jcat.2006.11.006
30. Nandan, D., et al., Acid functionalized carbon-silica composite and its application for Solketal production. Microporous and Mesoporous Materials, 2013. 179: p. 182-190. Doi.org/10.1016/j.micromeso.2013.06.004
31. Nanda, M., et al., A new continuous flow process for catalytic conversion of glycerol to oxygenated fuel additive: Catalyst screening. Applied Energy, 2014. 123: p. 75-81. Doi.org/10.1016/j.apenergy.2014.02.055
32. Gonzalez, A.C., et al., Selective glycerol transformations to high value added products catalysed by aluminosilicate supported iron oxide nanoparticles. Catalysis Science & Technology, 2014. 4(12): p. 4242-4249. Doi: 10.1039/c4cy00714j
33. Zaher, S., et al., Green acetalization of glycerol and carbonyl catalyzed by $FeCl_3{\cdot}6H_2O$. Molecular Catalysis, 2017. 438: p. 204-213. Doi.org/10.1016/j.mcat.2017.06.006
34. Mahreni, M.M. Azimatun Nur, Investigation of ferri-alginate (fe-alg) as environmentally friendly catalyst on the formation of Solketal from glycerol and acetone. IOP Conference Series: Materials Science and Engineering, 2020. 742. Doi: 10.1088/1757-899X/742/1/012010
35. Prinsen, P., et al., Zeolite catalyzed palmitic acid esterification. Microporous and Mesoporous Materials, 2018. 262: p. 133-139. Doi: 10.1016/j.micromeso.2017.11.029
36. Pires, E.L., et al., Effects of oxidant and solvent on the liquid-phase cyclohexane oxidation catalyzed by Ce-exchanged zeolite Y. Applied Catalysis A: General 2000. 203: p. 231-237. PII: S0926-860X(00)00496-8
37. Silva, D., et al., Iron (III) silicotungstate: an efficient and recyclable catalyst for converting glycerol to Solketal. Energy & Fuels, 2020. 34(8): p. 9664-9673. Doi.org/10.1021/acs.energyfuels.0c01446
38. Esposito, R., et al., Iron(III) complexes for highly efficient and sustainable ketalization of glycerol: A combined experimental and theoretical study. ACS Omega, 2019. 4(1): p. 688-698. Doi: 10.1021/acsomega.8b02546
39. Delidovich, I., et al., Catalytic versus stoichiometric reagents as a key concept for Green Chemistry. Green Chemistry, 2016. 18(3): p. 590-593. Doi: 10.1039/c5gc90070k
40. Jackson, W., et al., Closing Pandora's box: Chemical products should be designed to preserve efficacy of function while reducing toxicity. Green Chemistry, 2016. Doi: 10.1039/c6gc90073a
41. Jessop, P., The use of auxiliary substances (e.g. solvents, separation agents) should be made unnecessary wherever possible and innocuous when used. Green Chemistry, 2016. 18(9): p. 2577-2578. Doi: 10.1039/c6gc90039a
42. Keshavarz1, A., et al., The effect of sulfuric acid, oxalic acid, and their combination on the size and regularity of the porous Al_2O_3 by anodization. Journal of Nanostructure in Chemistry, 2013. 3(34): p. 34-38. Doi: 10.1186/2193-8865-3-34

Scheme 1

Scheme 1 is available in the Supplementary Files section.

Figures

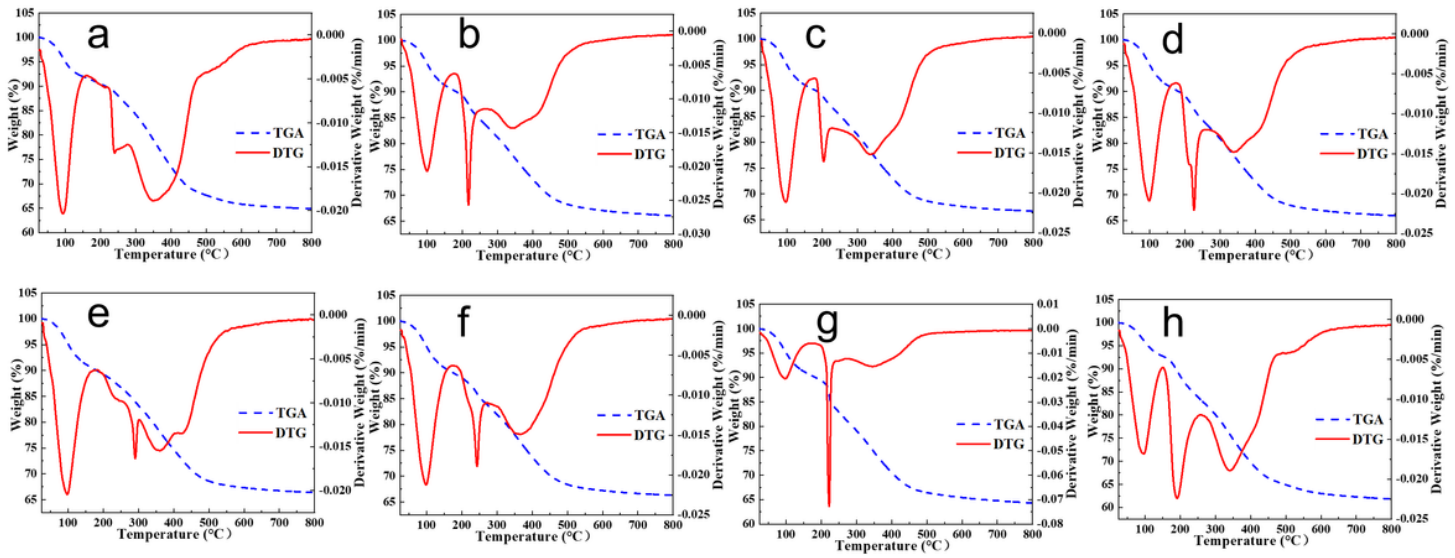

Figure 1

TGA and DTG curves of the precursors: (a) AlOOH-H_2O, (b) AlOOH-MT, (c) AlOOH-EA, (d) AlOOH-IPA, (e) AlOOH-NBA, (f) AlOOH-IAA, (g) AlOOH-HA, and (h) AlOOH-CA.

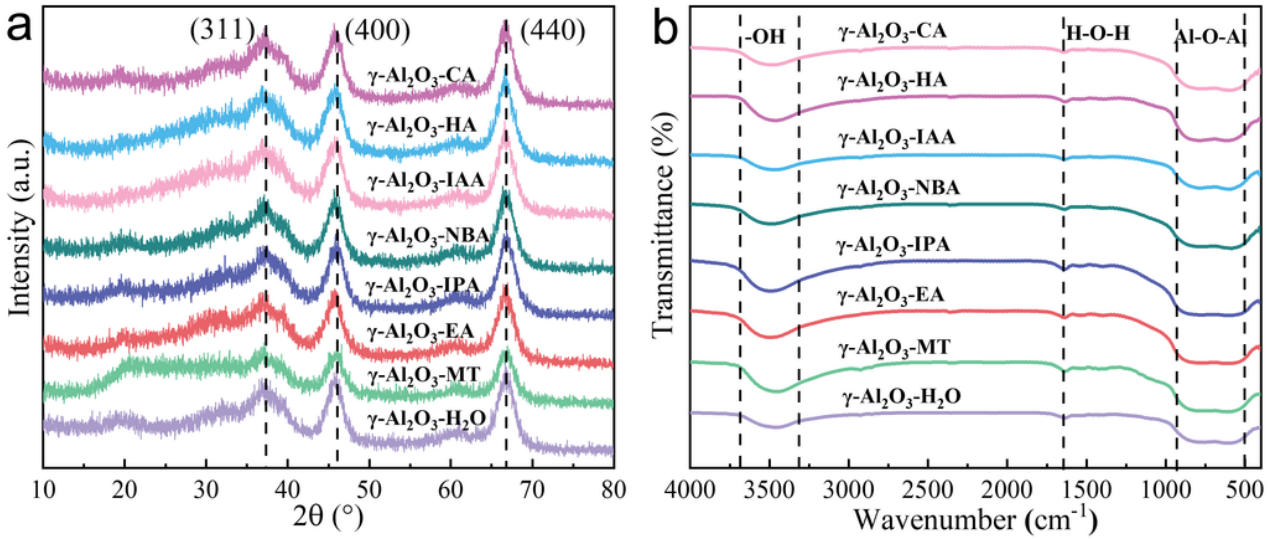

Figure 2

(a) XRD patterns, and (b) FTIR spectra of the various spherical γ-Al_2O_3.

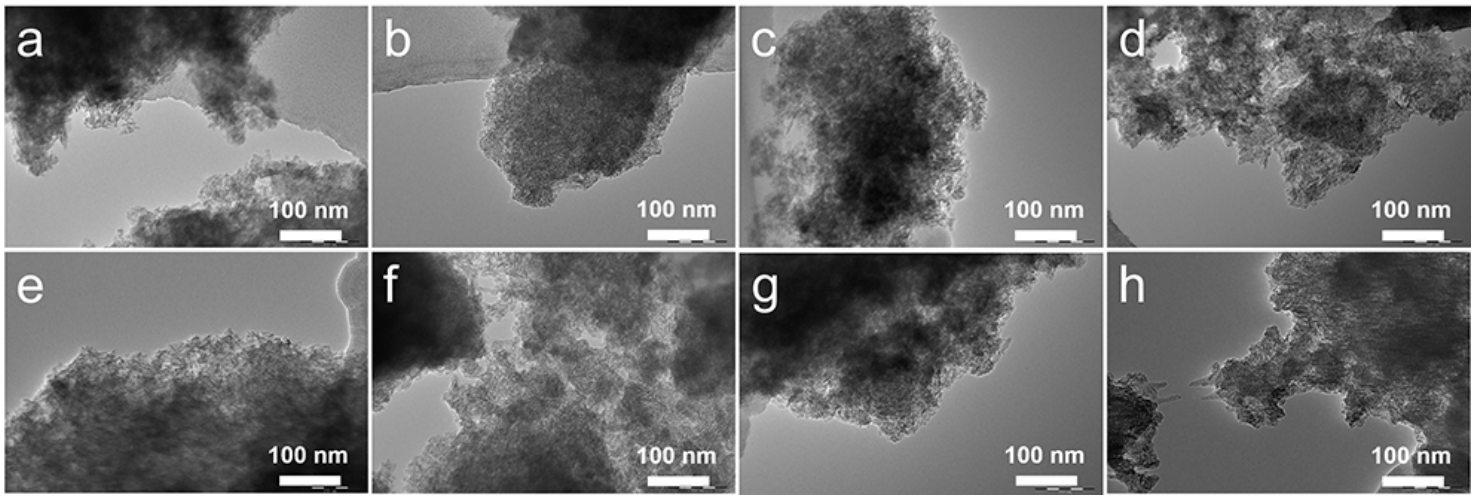

Figure 3

TEM images of (a) γ-Al_2O_3-H_2O, (b) γ-Al_2O_3-MT, (c) γ-Al_2O_3-EA, (d) γ-Al_2O_3-IPA, (e) γ-Al_2O_3-NBA, (f) γ-Al_2O_3-IAA, (g) γ-Al_2O_3-HA, and (h) γ-Al_2O_3-CA.

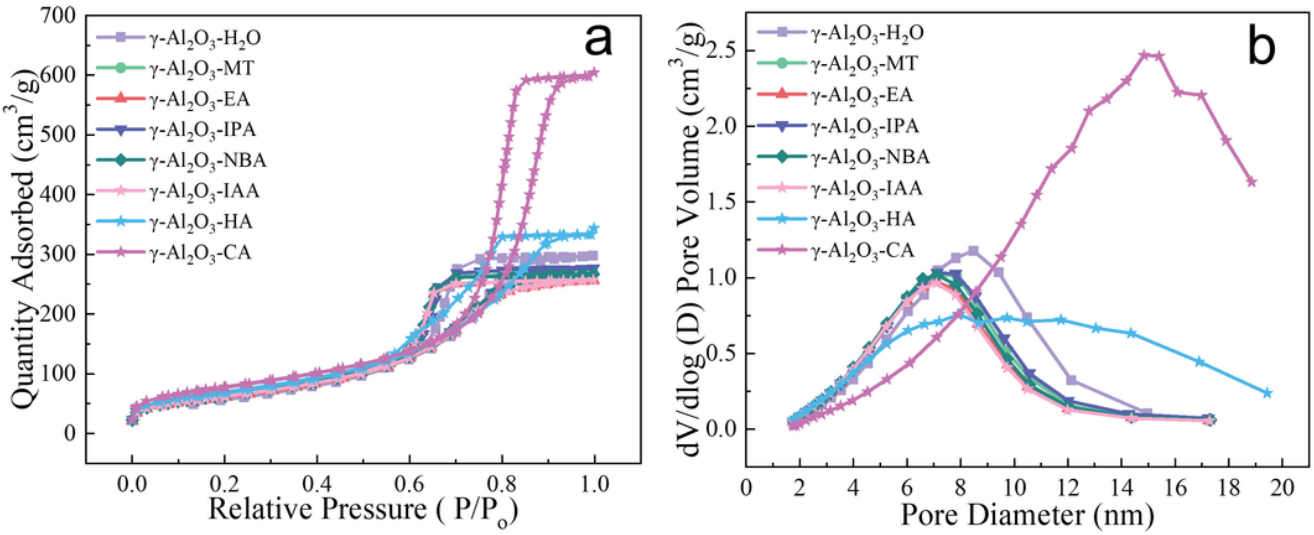

Figure 4

(a) Nitrogen adsorption-desorption isotherms, and (b) pore size distribution of the various spherical γ-Al_2O_3.

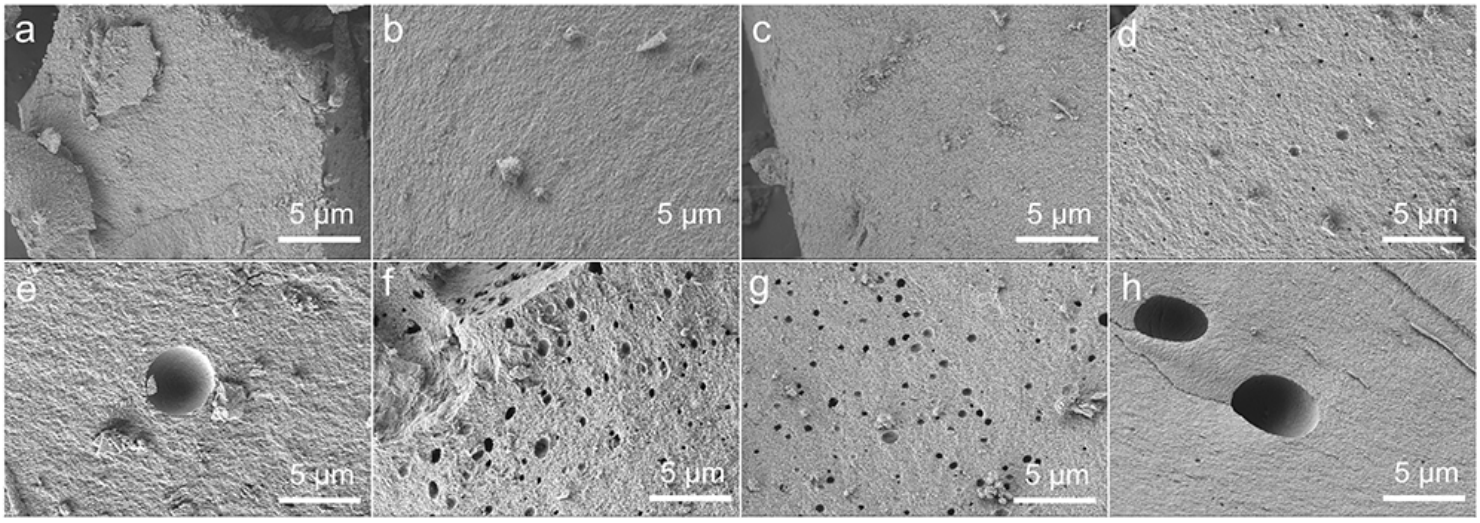

Figure 5

SEM micrographs of (a) γ-Al_2O_3-H_2O (b) γ-Al_2O_3-MT (c) γ-Al_2O_3-EA (d) γ-Al_2O_3-IPA (e) γ-Al_2O_3-NBA (f) γ-Al_2O_3-IAA (g) γ-Al_2O_3-HA (h) γ-Al_2O_3-CA.

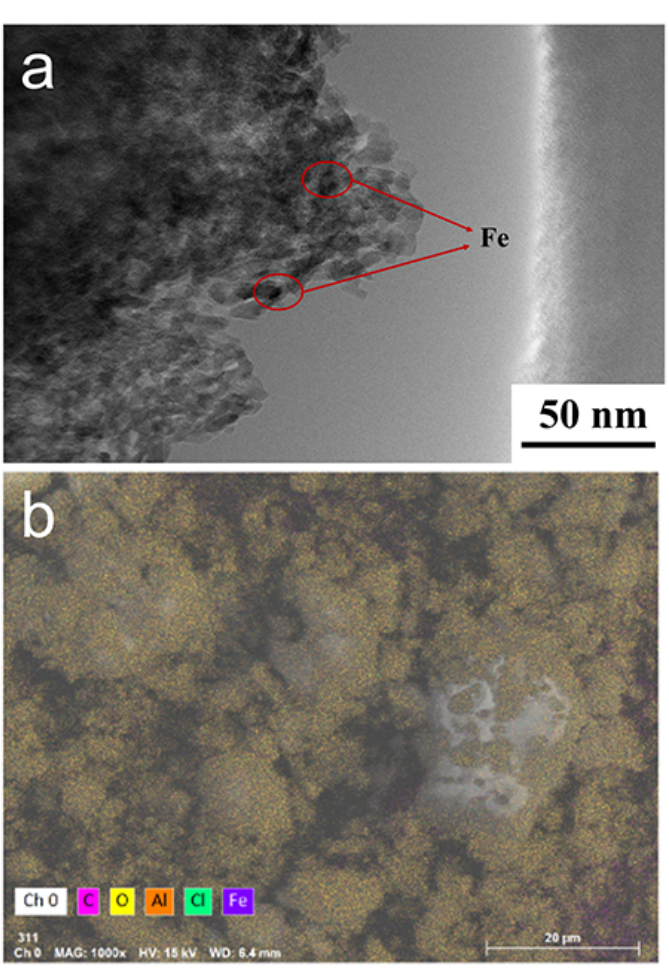

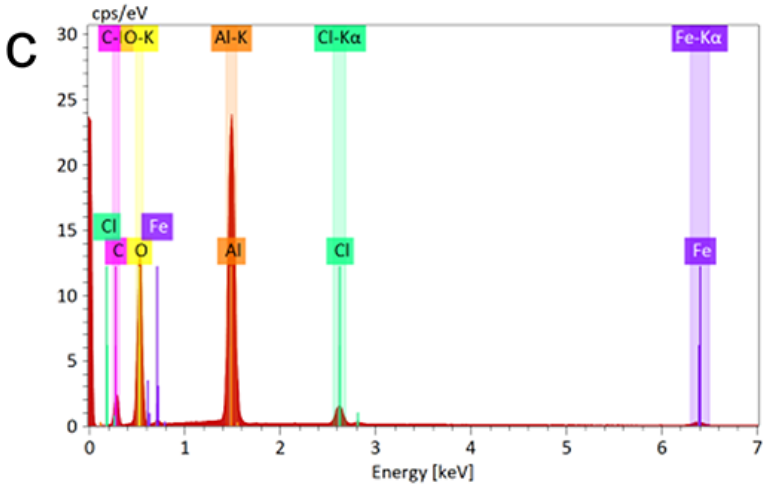

d

Element	Atomic number	Normalized quality / %	Atom / %	abs. error / % (1 sigma)
C	6	19.73	28.94	2.59
O	8	44.84	49.37	4.95
Al	13	29.35	19.16	1.34
Fe	26	2.75	0.87	0.12
Cl	17	3.33	1.65	0.14
		100.00	**100.00**	

Figure 6

(a) TEM image, (b-d) EDS analysis of $FeCl_3$/γ-Al_2O_3-IPA.

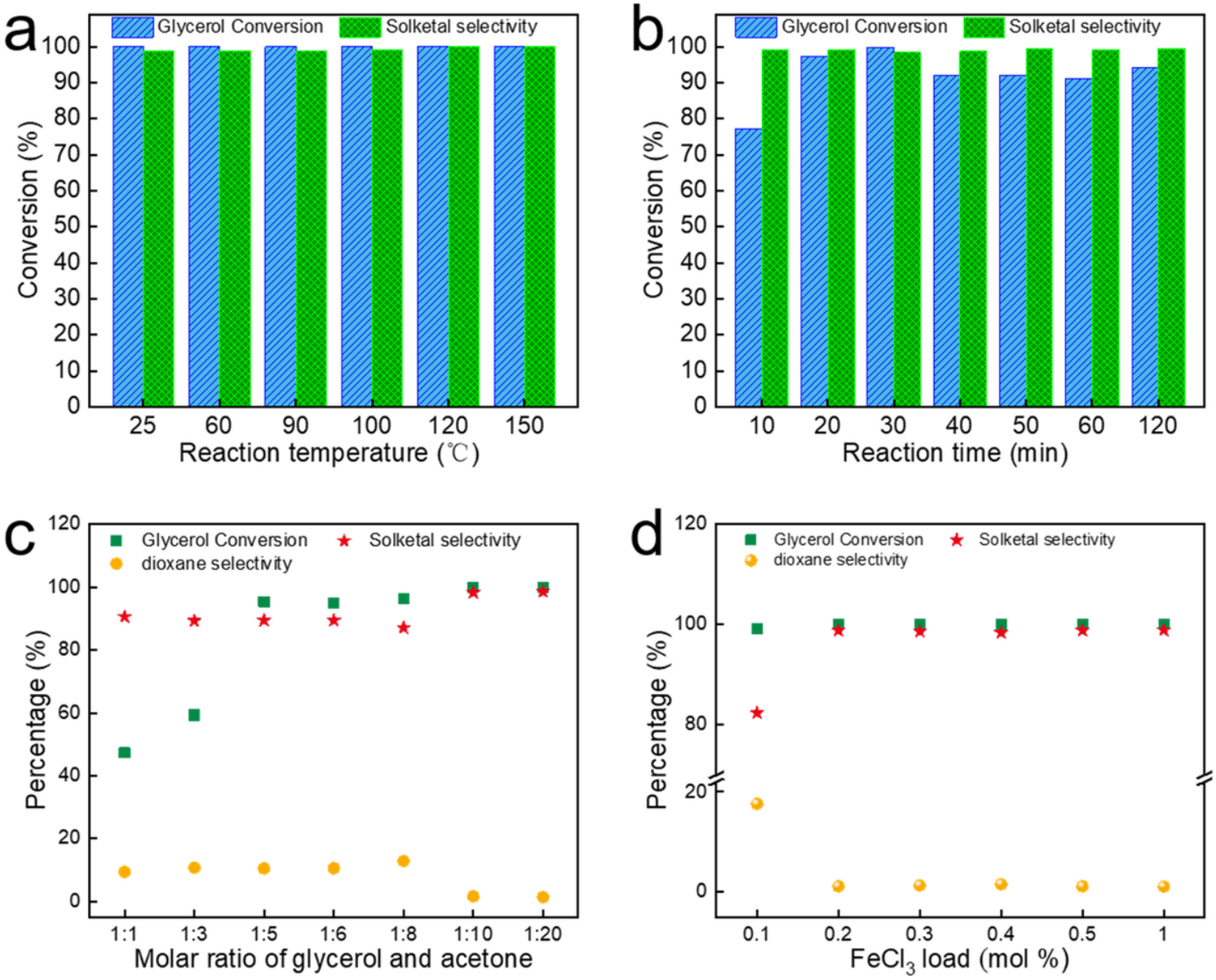

Figure 7

Effect of (a) the reaction temperature (10 mmol glycerol, 100 mmol acetone, 1 mol% $FeCl_3$/γ-Al_2O_3-IPA, 30 min), (b) the reaction time (10 mmol glycerol, 100 mmol acetone, 1 mol% $FeCl_3$/γ-Al_2O_3-IPA, 25 °C), (c) the molar ratio of glycerol and acetone (1 mol% $FeCl_3$/γ-Al_2O_3-IPA, 25 °C, 30 min), and (d) the $FeCl_3$ load (10 mmol glycerol, 100 mmol acetone, 25 °C, 30 min) on the glycerol conversions, Solketal selectivity, and/or Solketal yield of the acetalization reaction.

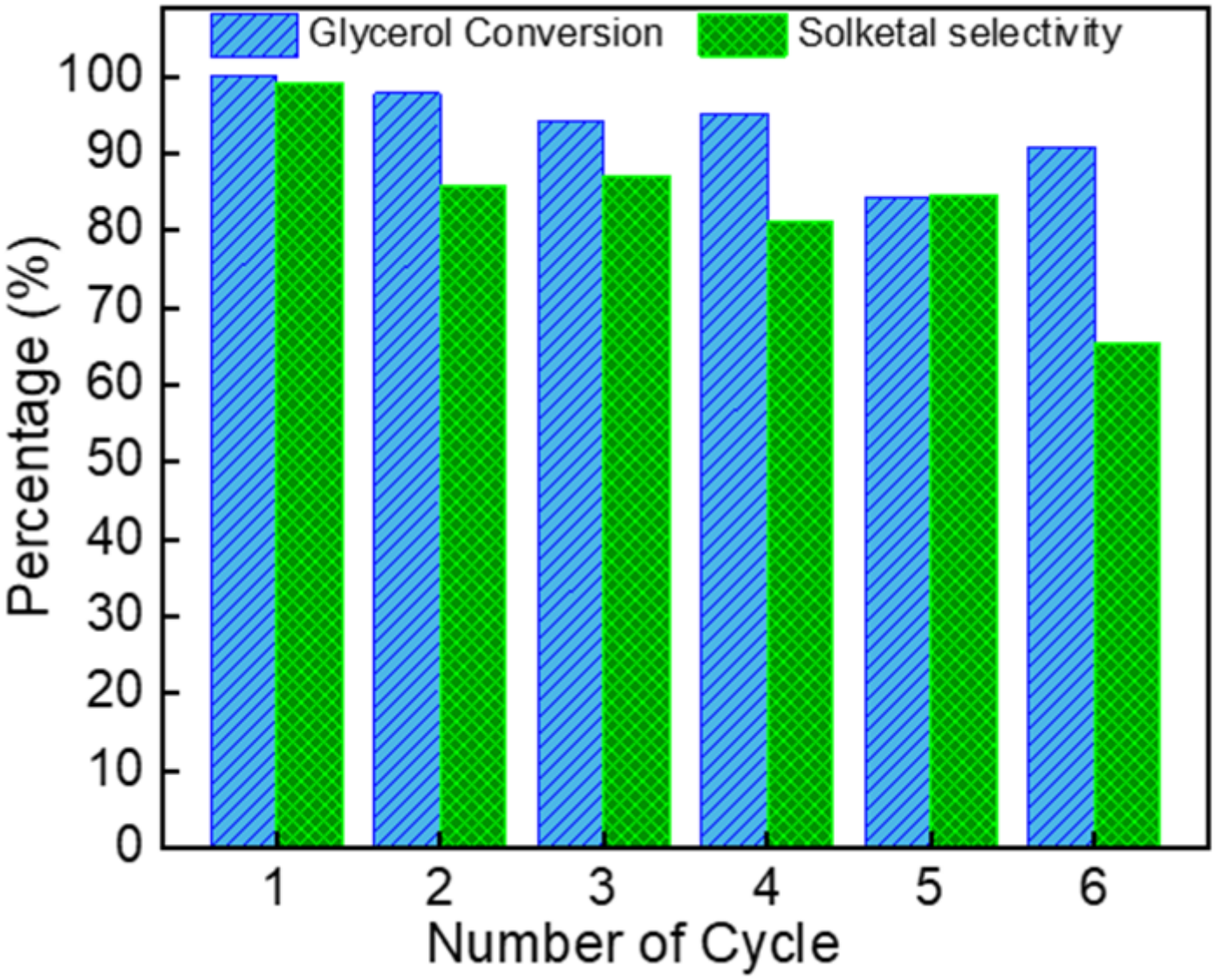

Figure 8

Catalytic performance of the recycled $FeCl_3$/γ-Al_2O_3-IPA.

Supplementary Files

This is a list of supplementary files associated with this preprint. Click to download.

- GraphicalAbstract.tif
- Scheme1.tif